

Intermediate coupling in $^{203,205}\text{Tl}^\dagger$

J. M. Davidson,* P. W. Green, H. R. Hooper, D. M. Sheppard, and G. C. Neilson

Nuclear Research Centre, The University of Alberta, Edmonton, Alberta, Canada T6G 2N5

(Received 16 September 1976)

The excited states of $^{203,205}\text{Tl}$ were studied using the $^{203,205}\text{Tl}(n, n'\gamma)$ reactions. γ -ray angular distributions were measured and spin assignments were made for excited states in both nuclei. An intermediate coupling model calculation was performed in which these nuclei were represented by the coupling of a single hole in the $3s_{1/2}$, $2d_{3/2}$, $2d_{5/2}$, and $1g_{7/2}$ proton shells to the quadrupole vibrations of the appropriate Pb core. The results of these calculations were compared with the experimental results of this and previous works.

[NUCLEAR REACTIONS $^{203, 205}\text{Tl}(n, n'\gamma)$, $E=1.03\text{--}2.26$ MeV; measured E_γ , $\sigma(E_\gamma, \theta_\gamma)$; $^{203, 205}\text{Tl}$ deduced levels, J , π , δ . Intermediate coupling model calculation. Enriched and natural targets. Ge(Li) detectors.]

I. INTRODUCTION

It has often been suggested that the low-lying states of $^{203,205}\text{Tl}$ are well represented by the intermediate coupling of a single hole in the closed $Z=82$ proton system to the vibrational states of the appropriate Pb core. A number of theoretical calculations for these nuclei are reported in the literature,¹⁻⁴ and the results are in good agreement with the known⁵ properties of the ground and first two excited states. A more extensive test of the intermediate coupling model (ICM) in $^{203,205}\text{Tl}$ has been limited in earlier works by the lack of any levels at higher excitation energy that can be firmly identified with those predicted by theory.

In order to identify further levels in the experimental spectra of these nuclei with those predicted by the ICM, a more extensive knowledge of level spins is necessary. In previous works, the study of charged-particle reactions⁶⁻⁸ and the inelastic scattering of neutrons^{9,10} and photons¹¹⁻¹³ has established angular momentum transfers, spectroscopic factors and γ -ray branching ratios for many levels. However, few spins are known above the second excited state, and γ -ray angular distributions, which are useful in determining spins, have not been reported.

In the present work, the excited states of $^{203,205}\text{Tl}$ were studied using the $^{203,205}\text{Tl}(n, n'\gamma)$ reactions. γ -ray angular distributions were measured and spins or spin limits were deduced for excited states in both nuclei. An ICM calculation was performed in which a single hole in the $3s_{1/2}$, $2d_{3/2}$, $2d_{5/2}$, and $1g_{7/2}$ proton shells was coupled to the quadrupole vibrations of a $^{204,206}\text{Pb}$ core. Excitation energies, spectroscopic factors, and transi-

tion rates were calculated and compared to the results of this and previous works. Preliminary reports of this study have been given.¹⁴

II. EXPERIMENTAL DETAILS

γ -ray angular distributions from the $^{203,205}\text{Tl}(n, n'\gamma)$ reactions were recorded using a small-sample technique.¹⁵ Neutrons were produced using the $^7\text{Li}(p, n)^7\text{Be}$ and $^3\text{H}(p, n)^3\text{He}$ reactions. The lithium target consisted of a ~ 1 mg/cm² layer of Li_2CO_3 evaporated onto a gold backing. The tritium target consisted of a 3.27 mg/cm² layer of metallic erbium deposited on a tantalum backing with tritium absorbed in the erbium layer at a 1:1 atomic ratio. Maximum neutron energies in different runs ranged from 1.03 to 2.26 MeV. A 10 ns pulsed proton beam with a 1 MHz repetition rate was provided by the University of Alberta Van de Graaff accelerator. The pulsed beam enabled the use of time-of-flight gating to reduce background in the γ -ray spectra. Average beam currents were typically 0.5 μA and the accumulated charge per angle was typically 10 mC. The thallium scatterers consisted of compressed cylinders of isotopically enriched Tl_2O_3 of total mass 11.1 g in the case of ^{203}Tl (> 95% ^{203}Tl) and 3.25 g for ^{205}Tl (> 97% ^{205}Tl) and of a 1.3 cm \times 1.3 cm diam cylinder of natural thallium metal (29.5% ^{203}Tl and 70.5% ^{205}Tl). The scatterer was positioned so that its axis and the beam axis were collinear. The distance from the 0.32 cm diam circular beamspot to the base of the scatterer was typically 0.7 cm. γ rays were detected in Ge(Li) detectors placed approximately 50 cm from the scatterer. A ^{137}Cs γ -ray source was placed near the Ge(Li) detector to provide a

monitor of system gain stability and dead time. Neutron total flux was monitored using a stationary NE213 liquid scintillator placed several meters from the target. Signals from the detectors were analyzed and stored in an on-line computer.

A typical γ -ray spectrum is shown in Fig. 1.

III. EXPERIMENTAL RESULTS AND ANALYSIS

The γ -ray decays of levels in $^{203,205}\text{Tl}$ as observed in the present work are shown as solid lines in Figs. 2 and 3. Other transitions reported for these levels,⁵ but not seen in the present work, are indicated in these figures by dashed lines.

The γ -ray angular distributions were analyzed using the computer code EVA,^{15,16} which applies corrections for finite beam spot and scatterer size to the theoretical angular distributions and compares them to the data using a χ^2 test.

The alignment of initial states in the γ decays was calculated using the statistical compound nuclear model (see, e.g., Ref. 17). The optical model parameters were those of Wilmore and Hodgson.¹⁸ Plots of χ^2 were generated as a function of the initial state spin J_i and the multipole mixing ratio δ . Minima in $\chi^2(J_i, \delta)$ falling above the 0.1% confidence limit were ruled out as corresponding to possible combinations of J_i and δ for that tran-

sition.¹⁹ Minima falling below this limit, and not otherwise ruled out (e.g., from the results of earlier works), are listed in Tables I and II. The errors on the mixing ratios were calculated following the $\chi^2_{\text{min}} + 1$ rule.²⁰ The signs of the mixing ratios are in accordance with the phase convention of Rose and Brink.²¹ An upper limit of approximately 10 ns was placed on the lifetimes of all $^{203,205}\text{Tl}$ excited states seen in this work, because their deexcitation γ rays were observed only in coincidence with the prompt beam burst. This upper limit enabled the rejection of some initial state spin-parity combinations for transitions which required nonzero values of δ to fit the experimental data.²²

A sample γ -ray angular distribution and χ^2 plot are shown in Figs. 4 and 5, respectively.

IV. DISCUSSION OF EXPERIMENTAL RESULTS

Seventeen states have been reported^{5,10} in ^{203}Tl and 10 states have been reported⁵ in ^{205}Tl below 1.5 MeV excitation. In the present work, spins or spin limits are deduced for several of these levels on the basis of χ^2 tests combined with the results of earlier works.

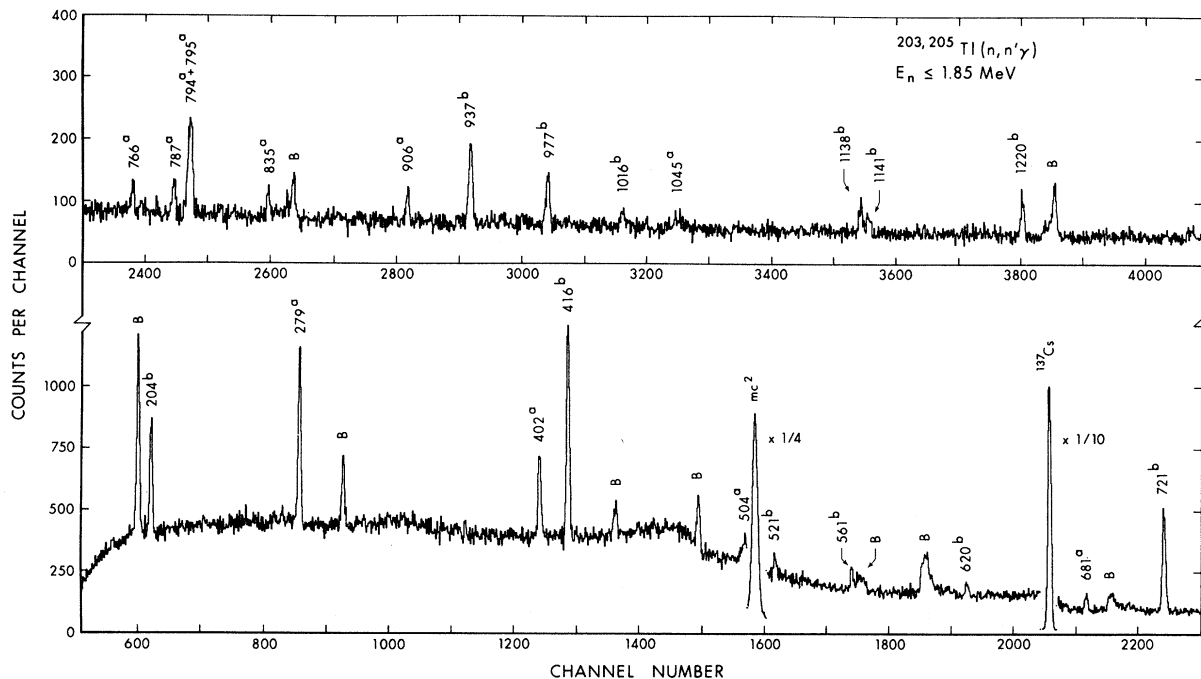


FIG. 1. A γ -ray spectrum from the $(n, n'\gamma)$ reaction on natural thallium is shown; γ -ray energies are given in keV and the superscripts denote the source of the γ rays to be (a) ^{203}Tl and (b) ^{205}Tl , respectively. Background peaks are denoted by a B.

A. Excited states of ^{203}Tl

1. Levels at 279 and 681 keV

The spin-parities of these levels have been established⁵ to be $\frac{3}{2}^+$ and $\frac{5}{2}^+$, and the reported⁵ values of $\arctan\delta$ for the 279-0 and 681-279 keV transitions are $50^\circ \pm 5^\circ$ and $3^\circ \pm 1^\circ$, respectively. The values of $\arctan\delta$ deduced in this work are $-60^\circ \pm 5^\circ$ and $2^\circ \pm 8^\circ$, in good agreement with the earlier values, where the sign of the mixing ratio is reversed due to the use of a different phase convention in the earlier works. The angular distribution of the 681-0 keV transition is consistent with the initial state assignment of $\frac{5}{2}^+$.

2. Level at 1045 keV

The angular distribution of the 1045-279 keV transition is consistent with assignments of $\frac{3}{2}$, $\frac{5}{2}$, and $\frac{7}{2}$ for this level. The choice of $\frac{7}{2}$ may be ruled

out, because the 1045-0 keV transition would then have a strength of ≥ 50 Weisskopf units most unlikely for an $E3$ transition.²² Of the remaining choices, $\frac{5}{2}$ is slightly favored, because the 1045 keV level was not seen in a previous $^{203}\text{Tl}(\gamma, \gamma')$ study.¹² In that work, the assumed $E1$ primary decay transitions of the 6418 keV resonance level ($J^\pi = \frac{1}{2}^+$) selected out lower-lying ^{203}Tl levels of $J^\pi = \frac{1}{2}^+$ and $\frac{3}{2}^+$, but not levels of $J > \frac{3}{2}$.

3. Level at 1066 keV

The angular distribution of the 1066-279 keV transition is consistent with assignments of $\frac{3}{2}$, $\frac{5}{2}$, and $\frac{7}{2}$, although only at the 0.7% confidence level in the case of $\frac{3}{2}$. The choice of $\frac{5}{2}$ may be slightly favored from the relatively low (10%) confidence level for $\frac{7}{2}$. The fact that the level was not observed in $^{203}\text{Tl}(\gamma, \gamma')$ is consistent with its having a spin of $J > \frac{5}{2}$.

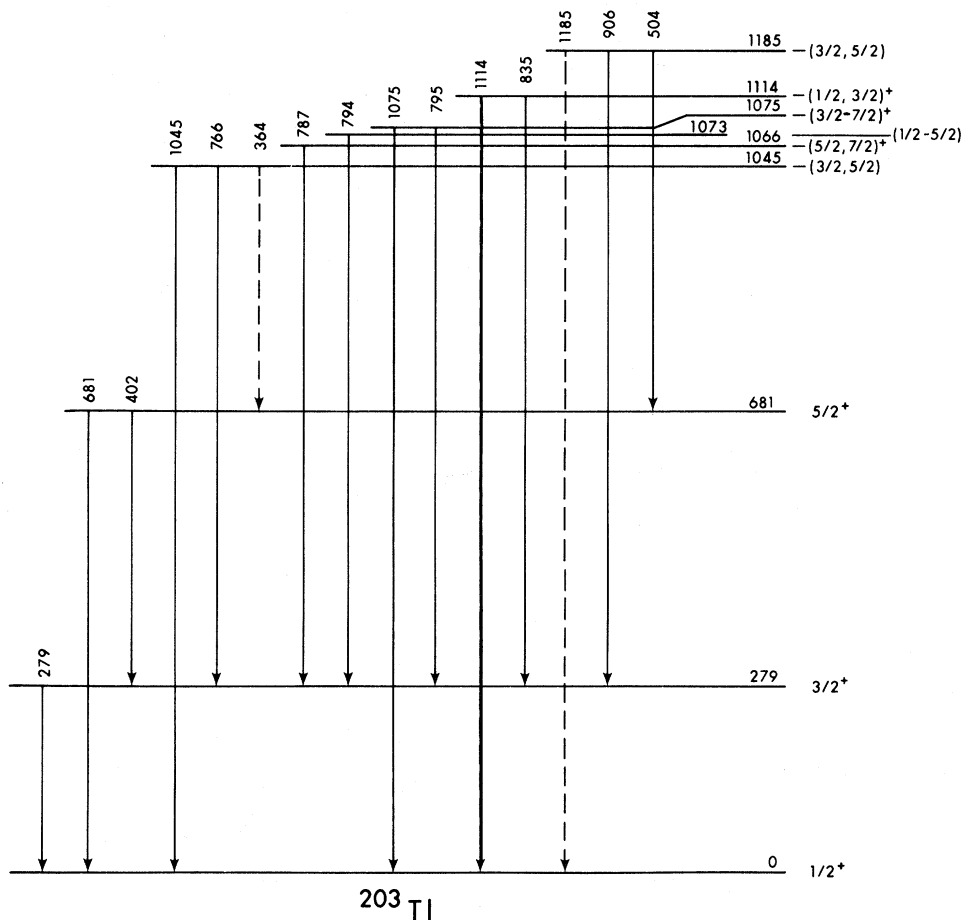


FIG. 2. The level and decay scheme of ^{203}Tl is shown. Transitions observed in the present work are shown as solid lines, while the dashed lines indicate previously reported transitions which were not seen in this work. Level and transition energies are given in keV and adopted level spins are given at the right side of the figure.

4. Levels at 1073 and 1075 keV

A previously reported ^{203}Tl level at 1074 keV excitation is shown in the present work to be a doublet. Figure 6 shows an expanded portion of a γ -ray spectrum from the $^{203}\text{Tl}(n, n'\gamma)$ reaction which includes the peaks from the 1073–279 and 1075–279 keV transitions. The widths of the peaks noted in that figure were obtained by fitting a single Gaussian shape to each peak. The peak near 795 keV has a significantly larger width than do the other two peaks in the figure and a small dip is visible between the indicated locations of the two member peaks, indicating that the 795 keV peak is a γ -ray doublet. The larger width of the 795 keV γ ray is not due to an intrinsically large width of the initial state, because it lies below the thresholds for particle emission. It is not due to Doppler broadening,

because the low energy of the neutrons and the high mass of the ^{203}Tl scatterer nuclei limit Doppler shifts to smaller values than would be required to account for the observed broadening. The positions of the members of this γ -ray doublet were determined by fitting two Gaussian shapes of fixed width to the experimental peak shapes. The resulting separation of the two γ rays is 1.4 ± 0.1 keV and the separation of the lower doublet member from the γ ray near $E_\gamma = 787$ keV is 7.2 ± 0.2 keV. Based on the reported⁹ energy of 786.8 ± 0.5 keV for that γ ray, and on an excitation energy of 279.2 keV for the ^{203}Tl first excited state,⁵ the corresponding excitation energies of the members of the doublet are 1073.2 ± 0.5 and 1074.6 ± 0.5 keV.

The angular distribution data for the 1073–279 and 1075–279 keV transitions is consistent with assignments of $\frac{1}{2}$, $\frac{3}{2}$, and $\frac{5}{2}$ for the 1073.2 keV level

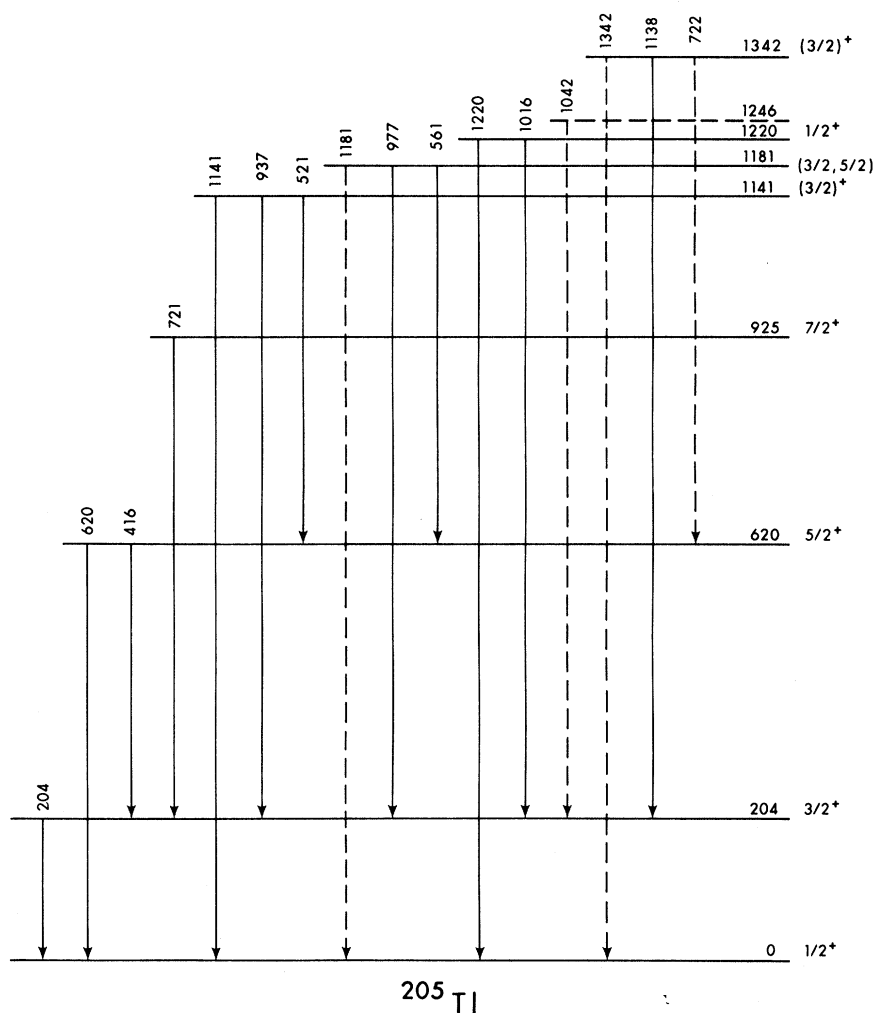


FIG. 3. The level and decay scheme of ^{205}Tl is shown. The notation is as described for Fig. 2.

TABLE I. Experimental J^π values and mixing ratios in ^{203}Tl .

Level energy ^a	γ -ray energy ^a	$J_i^\pi \rightarrow J_f^\pi$	Arctan δ ^b	Confidence level ^c
279	279	$\frac{3}{2}^+ \rightarrow \frac{1}{2}^+$	-60 <u>5</u>	
681	681	$\frac{5}{2}^+ \rightarrow \frac{1}{2}^+$	0 ^d	
	402	$\rightarrow \frac{3}{2}^+$	2 <u>8</u>	
1045	766	$\frac{3}{2} \rightarrow \frac{3}{2}^+$	-38 <u>35</u>	
		$\frac{5}{2}^+ \rightarrow$	-76 <u>12</u>	
1066	787	$\frac{3}{2}^+ \rightarrow \frac{3}{2}^+$	-38 <u>22</u>	0.7
		$\frac{5}{2}^+ \rightarrow$	-70 <u>11</u>	
		\rightarrow	-37 <u>11</u>	
1073	794	$\frac{7}{2}^+ \rightarrow$	0 ^d	10
		$\frac{1}{2} \rightarrow \frac{3}{2}^+$	All	
		$\frac{3}{2} \rightarrow \frac{3}{2}^+$	28 <u>32</u>	
		\rightarrow	76 <u>32</u>	
		$\frac{5}{2} \rightarrow$	-6 <u>12</u>	
1075	796	$\frac{3}{2}^+ \rightarrow \frac{3}{2}^+$	-38 <u>26</u>	
		$\frac{5}{2}^+ \rightarrow$	-76 <u>8</u>	
		\rightarrow	-30 <u>8</u>	
		$\frac{7}{2}^+ \rightarrow$	0 ^d	
1185	906	$\frac{3}{2} \rightarrow \frac{3}{2}^+$	-64 <u>24</u>	
		\rightarrow	-11 <u>24</u>	
		$\frac{5}{2}^+ \rightarrow$	-86 <u>12</u>	
		\rightarrow	-21 <u>10</u>	
		$\frac{7}{2}^+ \rightarrow$	0 ^d	

^a The energies are in keV from Refs. 9 and 10 and the present work. The uncertainties are ± 0.5 keV.

^b Arctan δ is given in degrees. The underlined numbers give the uncertainties, referring to the last quoted significant figures. The phase convention of Rose and Brink (Ref. 21) has been used.

^c The confidence level is given as a percentage for all cases where it is $\leq 10\%$.

^d The radiation was assumed to be pure quadrupole (see Sec. III).

and $\frac{3}{2}$, $\frac{5}{2}$, and $\frac{7}{2}$ for the 1074.6 keV state. The fact that neither is seen¹² in $^{203}\text{Tl}(\gamma, \gamma')$ is consistent with assignments of $J > \frac{3}{2}$ in both cases, although it does not rule out $J \leq \frac{3}{2}$. A γ ray of energy 1074.9 ± 0.5 keV was reported in an earlier work⁹ to arise from a 7% ground state decay branch of a 1074 keV level, assumed a singlet. If that γ ray were from the decay of the 1074.6 keV level, then a spin of $\frac{7}{2}$ for that level would be unlikely, because

TABLE II. Experimental J^π values and mixing ratios in ^{205}Tl .

Level energy ^a	γ -ray energy ^a	$J_i^\pi \rightarrow J_f^\pi$	Arctan δ ^b	Confidence level ^c
204	204	$\frac{3}{2}^+ \rightarrow \frac{1}{2}^+$	-60 <u>22</u>	
620	416	$\frac{5}{2}^+ \rightarrow \frac{3}{2}^+$	-5 <u>7</u>	
925	721	$\frac{7}{2}^+ \rightarrow \frac{3}{2}^+$	0 ^d	
1141	1141	$\frac{1}{2} \rightarrow \frac{1}{2}^+$	0 ^e	1.4
		$\frac{3}{2}^+ \rightarrow \frac{1}{2}^+$	-88 <u>22</u>	
		\rightarrow	-32 <u>22</u>	
1066	787	$\frac{3}{2}^+ \rightarrow$	0 ^d	
		$\frac{1}{2} \rightarrow \frac{3}{2}^+$	All	
		$\frac{3}{2} \rightarrow$	-89 <u>13</u>	
1073	794	\rightarrow	14 <u>13</u>	
		$\frac{3}{2}^+ \rightarrow$	-11 <u>7</u>	
		\rightarrow	83 <u>7</u>	
1181	977	$\frac{1}{2} \rightarrow \frac{3}{2}^+$	All	1
		$\frac{3}{2}^+ \rightarrow$	36 <u>24</u>	
		\rightarrow	69 <u>24</u>	
1075	796	$\frac{3}{2}^+ \rightarrow$	-4 <u>8</u>	
		\rightarrow	77 <u>8</u>	
1220	1220	$\frac{1}{2} \rightarrow \frac{1}{2}^+$	0 ^e	
1342	1138	$\frac{3}{2} \rightarrow \frac{3}{2}^+$	-55 <u>30</u>	
		\rightarrow	-20 <u>30</u>	
		$\frac{5}{2}^+ \rightarrow \frac{3}{2}^+$	-84 <u>11</u>	
		\rightarrow	-24 <u>11</u>	

^a The energies are in keV from Refs. 9 and 10 and the present work. The uncertainties are ± 0.5 keV.

^b Arctan δ is given in degrees. The underlined numbers give the uncertainties, referring to the last quoted significant figures. The phase convention of Rose and Brink (Ref. 21) has been used.

^c The confidence level is given as a percentage for all cases where it is $\leq 10\%$.

^d The radiation was assumed to be pure quadrupole (see Sec. III).

^e For a $\frac{1}{2} \rightarrow \frac{1}{2}$ transition, δ is rigorously zero.

of the large octupole strength that would be required (see Sec. IV A 2.). On the other hand, no γ ray of that energy was seen in the present work. Further, the relatively large strength of population of the 1074.6 keV ^{203}Tl state suggests, from a comparison to the ^{205}Tl level and decay scheme, that it corresponds to the $\frac{7}{2}^+$ ^{205}Tl level at 925 keV excitation which is also strongly populated (see Fig. 1 and Sec. IV B 2).

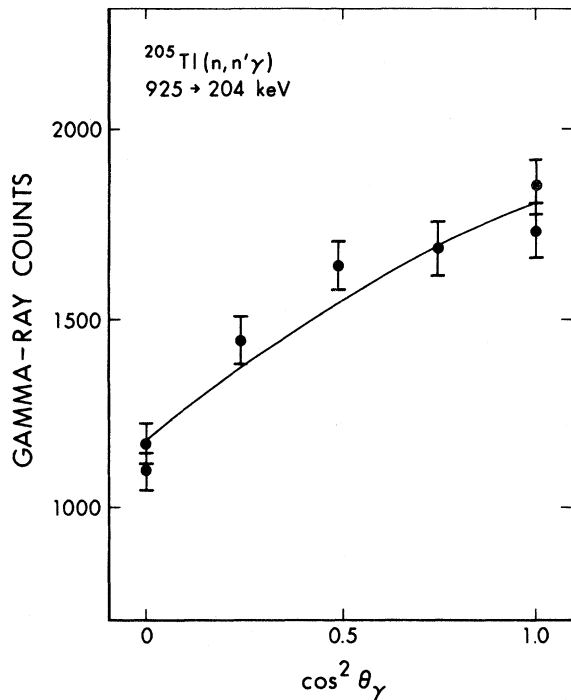


FIG. 4. A sample γ -ray angular distribution and theoretical curve generated by EVA (Ref. 16) are shown. The theoretical curve is for an initial state spin-parity of $\frac{7}{2}^+$; the final state is known (Ref. 5) to be $\frac{3}{2}^+$.

5. Level at 1114 keV

The γ rays from the 1114 \rightarrow 0 and 1114 \rightarrow 279 keV transitions were observed in this work. Angular distributions were not measured for either of these decays, because the strength of the γ ray from the

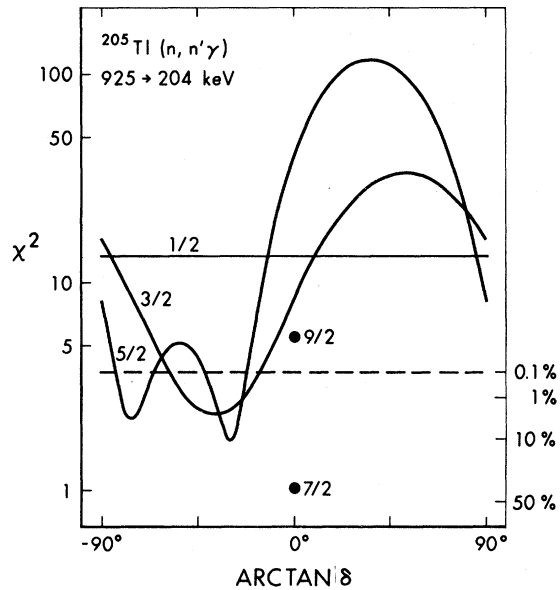


FIG. 5. Plots of χ^2 vs $\arctan \delta$ are shown for the data displayed in Fig. 4. An initial state spin of $\frac{7}{2}$ is preferred, although values of $\frac{3}{2}$ and $\frac{5}{2}$ are also acceptable. This result, combined with a previously reported (Ref. 8) limit of $J^\pi = (\frac{7}{2}, \frac{9}{2})^+$, determines the 924 keV state of ^{205}Tl to be $J^\pi = \frac{7}{2}^+$.

1114 \rightarrow 279 keV transition was obscured at forward angles by a background peak from $^{72}\text{Ge}(n, n'\gamma)$. This level is seen in $^{203}\text{Tl}(\gamma, \gamma')$, suggesting that it is $J^\pi = (\frac{1}{2}, \frac{3}{2})^+$.

6. Level at 1185 keV

The angular distribution data from the 1185 \rightarrow 279 keV transition is consistent with assignments of

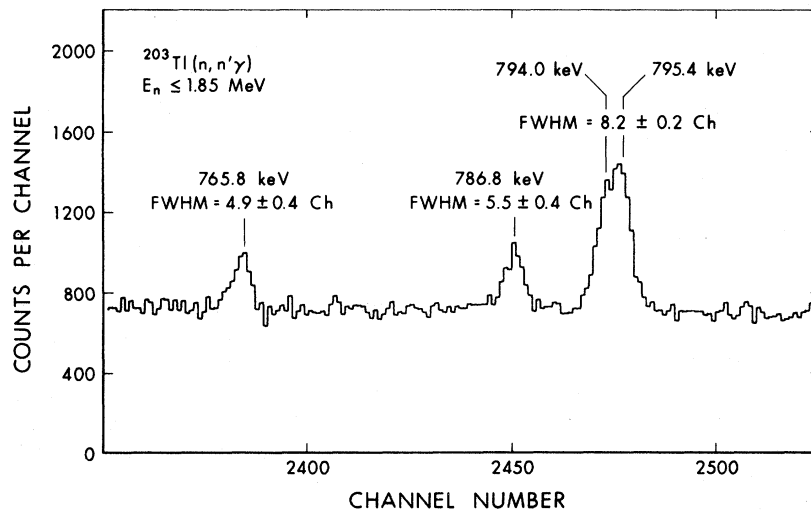


FIG. 6. An expanded portion of the γ -ray spectrum from the $^{203}\text{Tl}(n, n'\gamma)$ reaction is shown. The significantly larger width of the peak near $E_\gamma = 795$ keV indicates that it is a doublet.

$\frac{3}{2}$, $\frac{5}{2}$, and $\frac{7}{2}$ for this level, although a spin of $\frac{7}{2}$ is permitted at only the 4% confidence level. The angular distribution of the 1185–681 keV transition could not be measured because of the proximity of the 511 keV annihilation peak. A previously reported⁹ γ ray from the 1185–0 keV transition was not observed in this work, however, if a weak ground state decay branch does exist, then an assignment of $\frac{3}{2}$ or $\frac{5}{2}$ is favored over $\frac{7}{2}$ (see Sec. IV A 2). The absence¹² of this level in $^{203}\text{Tl}(\gamma, \gamma')$ is consistent with an assignment of $J > \frac{3}{2}$.

B. Excited states of ^{205}Tl

1. Levels at 204 and 620 keV

The spin-parities of these levels have been established⁵ to be $\frac{3}{2}^+$ and $\frac{5}{2}^+$, and the reported⁵ values of $\arctan\delta$ for the 204–0 and the 620–204 keV transitions are $55^\circ \pm 3^\circ$ and $0^\circ \pm 3^\circ$, respectively. The values of $\arctan\delta$ deduced in this work are $-60^\circ \pm 22^\circ$ and $-5^\circ \pm 7^\circ$, in good agreement with the earlier values, where, as noted previously, the sign of the mixing ratio is reversed due to the use of a different phase convention in the earlier works.

2. Level at 925 keV

This level was reported⁸ in $^{205}\text{Tl}(p, p')$ to have $\Delta L = 4$, limiting it to $J^\pi = (\frac{7}{2}, \frac{9}{2})^+$, and it was not seen¹¹ in $^{205}\text{Tl}(\gamma, \gamma')$, which is consistent with a spin of $J > \frac{3}{2}$. It was reported^{9,10} in $^{205}\text{Tl}(n, n'\gamma)$ to decay to the $\frac{3}{2}^+$ first excited state, rather than the $\frac{5}{2}^+$ second excited state, which favors the assignment of $\frac{7}{2}^+$ over $\frac{9}{2}^+$. In the present work, an assignment of $\frac{9}{2}^+$ for the ^{205}Tl 925 keV state is rejected on two grounds. First, the angular distribution of γ rays from the 925–204 keV transition is consistent with an initial state spin of $\frac{3}{2}$, $\frac{5}{2}$, and $\frac{7}{2}$, but not $\frac{9}{2}$ (see Figs. 4 and 5). Second, the upper limit of ~ 10 ns placed on the lifetime of this level (see Sec. IV) is four orders of magnitude too small²² for the 925–204 keV transition to be $M3$. Thus, the 925 keV level of ^{205}Tl is assigned $J^\pi = \frac{7}{2}^+$.

3. Level at 1141 keV

This level has been reported⁶ in $^{205}\text{Pb}(t, \alpha)$ to have $l_n = 2$, limiting it to $J^\pi = (\frac{3}{2}, \frac{5}{2})^+$. It was also seen¹¹ in $^{205}\text{Tl}(\gamma, \gamma')$, making the choice of $\frac{3}{2}^+$ strongly favored. In the present work, the angular distribution data from the 1141–0 and 1141–204 keV transitions limits the initial-state spin to be $\frac{1}{2}$, $\frac{3}{2}$, or $\frac{5}{2}$, with the choice of $\frac{1}{2}$ allowed at only the 1.4% confidence level.

4. Level at 1181 keV

This level has been reported previously only in $^{205}\text{Tl}(n, n'\gamma)$ studies.^{9,10} In this work the γ -ray angular distribution from the 1181–204 transition is consistent with initial state spins of $\frac{1}{2}$, $\frac{3}{2}$, and $\frac{5}{2}$, with the choice of $\frac{1}{2}$ permitted at only the 1% confidence level.

5. Level at 1220 keV

This level is reported⁶ in $^{206}\text{Pb}(t, \alpha)$ to have $l_n = 0$, which establishes its spin and parity to be $J^\pi = \frac{1}{2}^+$. In the present work the angular distribution data from the 1220–0 keV transition is consistent with assignments of $J^\pi = \frac{1}{2}$, $\frac{3}{2}$, or $\frac{5}{2}$, in agreement with the earlier assignment.⁶

6. Level at 1342 keV

This level is reported⁸ in $^{205}\text{Tl}(p, p')$ to have $\Delta L = 2$, limiting it to $J^\pi = (\frac{3}{2}, \frac{5}{2})^+$, and it was seen¹¹ in $^{205}\text{Tl}(\gamma, \gamma')$, making $\frac{3}{2}^+$ strongly favored. In the present work the angular distribution data from the 1342–204 keV transition is consistent with an assignment of $J = \frac{3}{2}$, $\frac{5}{2}$, or $\frac{7}{2}$.

V. INTERMEDIATE COUPLING MODEL CALCULATION

Theoretical calculations were performed for $^{203,205}\text{Tl}$ in which these nuclei were represented by the intermediate coupling of a single hole in the closed $Z = 82$ proton system to the quadrupole vibrations of a $^{204,206}\text{Pb}$ core. A detailed description of the ICM, including all relevant formulas used in the present calculations and the notation used throughout this paper, is given by Castel, Stewart, and Harvey.²³ The active proton shells included in the calculation were the $3s_{1/2}$, $2d_{3/2}$, $2d_{5/2}$, and $1g_{7/2}$ orbitals and the core was allowed to have excitations of up to three phonons. The only adjustable parameter was the hole-core coupling strength constant ξ . Values for parameters of the model were taken from previous experimental information as follows. For both nuclei, the single-hole energies ϵ_j were taken from the experimental energy spectrum²⁴ of ^{207}Tl , and the single phonon energy $\hbar\omega$ was taken to be the excitation energy of the 2^+ first excited state of the appropriate Pb core.²⁵ Two calculations were made for each Tl isotope. In the first, the two- and three-phonon multiplets of the core excited states were degenerate in energy, having excitation energies of $2\hbar\omega$ and $3\hbar\omega$, respectively. In the second calculation, a modified form of the ICM, proposed by Castel *et al.*,²³ was used, in which anharmonic terms are included in the Hamiltonian to account for the experimentally observed splitting of the two-phonon triplet. For ^{205}Tl , the parameters n_j ,

describing this splitting, were taken directly from the excitation energies of the known²⁵ 0_2^+ , 2_2^+ , and 4_1^+ levels in ^{206}Pb . In the case of ^{203}Tl , the choice of the core parameters is difficult, because not all members of the two-phonon multiplet in ^{204}Pb have been identified. For the purpose of this calculation, the first 4^+ level in ^{204}Pb was assumed to belong to the two-phonon triplet, and the 0^+ and 2^+ members were assumed to be the levels at 1584 and 1932 keV excitation, respectively.²⁵ The splitting of the three-phonon multiplet was not taken into account, because there is insufficient experimental information on $^{204,206}\text{Pb}$ to identify the members of this multiplet in either nucleus. The effect

TABLE III. Parameters used in the ICM calculations.

	^{203}Tl		^{205}Tl	
	Not split	Split	Not split	Split
$\hbar\omega$ (MeV)	0.899	0.899	0.803	0.803
$\epsilon_{a_{3/2}}$ (MeV)	0.35	0.35	0.35	0.35
$\epsilon_{a_{5/2}}$ (MeV)	1.67	1.67	1.67	1.67
$\epsilon_{g_{7/2}}$ (MeV)	3.48	3.48	3.48	3.48
η_{0^+}	0.0	-0.24	0.0	-0.55
η_{2^+}	0.0	0.15	0.0	-0.18
η_{4^+}	0.0	-0.55	0.0	0.10
ξ	1.5	1.25	2.5	3.2

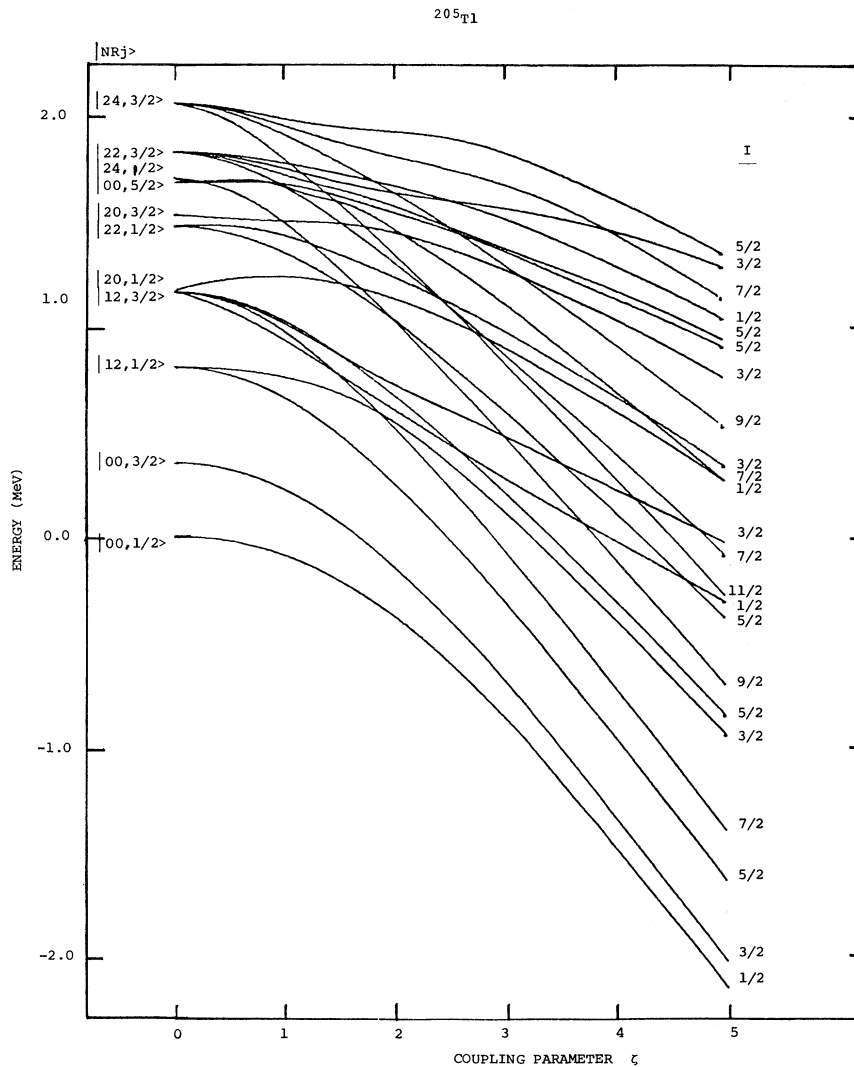


FIG. 7. Plots of calculated ^{205}Tl energy eigenvalues vs the hole-core coupling parameter are shown for the case of split vibrational multiplets in the ^{206}Pb core. For the noninteracting basis states $|NRj\rangle$ the labels denote a core state of N phonons coupled to an angular momentum R and a hole state of angular momentum j . The angular momentum to which R and j couple is labeled by I . All states shown have positive parity.

of this omission on the calculated energy levels below 1.5 MeV excitation is negligible, since no states in this region were found to have three-phonon core components of amplitude greater than ~ 0.2 . The model parameters used in the ICM calculations are listed in Table III.

For each parameter set, the matrix elements of the total Hamiltonian were calculated and the matrix was diagonalized for total spin values of $\frac{1}{2}$ to $\frac{11}{2}$ for a range of trial values of ξ . A sample plot of the low-lying energy eigenvalues as a function of ξ is shown in Fig. 7 for the case of ^{205}Tl . A best value of ξ was determined by finding that one which minimized the χ^2 deviation of calculated from experimental excitation energies. The values of ξ thus determined for the four parameter sets are also listed in Table III. The calculated excitation energies for some low-lying $^{203,205}\text{Tl}$ levels are given in Table IV and compared graphically to the experimental level schemes of $^{203,205}\text{Tl}$ in

Figs. 8 and 9. The spectroscopic strengths of these states are also listed in Table IV. The static moments of several low-lying states were calculated for values of $g_s = 5.58$ and $g_s = 3.50$ for the proton hole. The latter value of g_s is an effective value recommended by Covello and Sartoris.² The core gyromagnetic ratio was taken to be $g_R = Z/A$ and the quadrupole moments were calculated for an effective charge of $e_p = 1.0$. The results of the calculations for the static moments are listed in Table V. Reduced $M1$ and $E2$ transition rates were calculated for the electromagnetic decays of the low-lying states of $^{203,205}\text{Tl}$. The effective² value of $g_s = 3.50$ was also used in these calculations. The calculated values of level lifetimes are listed in Table VI. These values have been corrected for the contribution from conversion electron decay.²⁶ The calculated values of multipole mixing ratios and γ -ray branching ratios are given in Table VII. In all of the tables referred to in this subsection,

TABLE IV. Theoretical and experimental level energies and spectroscopic factors in $^{203,205}\text{Tl}$.

$(J^\pi)_i$ ^a	Energy ^b			$(2J+1)S$		
	Not split	Split	experiment ^c	Not split	Split	experiment ^c
^{203}Tl						
$(\frac{1}{2}^+)_1$	0.0	0.0	0.0	1.71	1.79	1.4
$(\frac{3}{2}^+)_1$	0.279	0.296	0.279	2.84	3.08	1.8
$(\frac{5}{2}^+)_1$	0.753	0.735	0.681	0.43	0.31	0.6
$(\frac{3}{2}^+)_2$	1.000	0.968		0.45	0.50	
$(\frac{7}{2}^+)_1$	1.035	0.923	1.075	0.10	0.06	
$(\frac{5}{2}^+)_2$	1.194	1.202		0.09	0.05	
$(\frac{3}{2}^+)_3$	1.247	1.249	1.233	0.58	0.35	0.7
$(\frac{1}{2}^+)_2$	1.253	1.211		0.21	0.15	
$(\frac{9}{2}^+)_1$	1.562	1.201	1.228	0.00	0.00	
^{205}Tl						
$(\frac{1}{2}^+)_1$	0.0	0.0	0.0	1.33	0.98	1.4
$(\frac{3}{2}^+)_1$	0.203	0.168	0.204	1.91	1.37	1.7
$(\frac{5}{2}^+)_1$	0.566	0.545	0.620	0.43	0.43	0.4
$(\frac{7}{2}^+)_1$	0.797	0.787	0.925	0.12	0.15	
$(\frac{3}{2}^+)_2$	0.963	0.991		0.15	0.02	
$(\frac{5}{2}^+)_2$	1.076	1.085		0.03	0.01	
$(\frac{1}{2}^+)_2$	1.196	1.191	1.220	0.47	0.66	0.2
$(\frac{3}{2}^+)_3$	1.257	1.405	1.141	1.58	1.97	0.8
$(\frac{9}{2}^+)_1$	1.284	1.341	1.434	0.00	0.00	

^a The subscript denotes whether the level is the first, second, etc., having that spin.

^b The energies are in MeV.

^c The experimental values are from the present works and Ref. 5.

the experimentally measured values corresponding to the calculated quantities are also given, wherever they are available.

VI. DISCUSSION OF THE THEORETICAL RESULTS

In this section we compare the results of our ICM calculations for $^{203,205}\text{Tl}$ to the combined experimental evidence provided by this and earlier works. The qualitative reproduction of the experimental evidence by the model is discussed, and several levels in the experimental $^{203,205}\text{Tl}$ level schemes are tentatively identified with predicted ones, thus providing an expanded basis on which to judge the validity of the ICM in $^{203,205}\text{Tl}$. The effect of introducing into the calculation the splitting of the two-phonon triplet in the $^{204,206}\text{Pb}$ cores is also discussed.

The agreement between the calculated and experimental properties for the $^{203,205}\text{Tl}$ ground and first two excited states, where the correspondence of experimental to theoretical levels is unambi-

guous, is generally good. The calculated excitation energies are in reasonable agreement with the experimental values. The large spectroscopic strengths in proton pickup reactions^{6,7} for the ground and first excited states are qualitatively well reproduced in both the normal and modified-core ICM calculations, although they are overestimated by about 50% and are actually predicted more accurately by the calculation which does not include the effect of the splitting of the two-phonon core multiplet. The spectroscopic strength of the second excited state is also in better agreement with the results from proton pickup^{6,7} for the normal ICM calculation. The ground state magnetic moment μ calculated using $g_s = 5.58$, is not well reproduced by the theory in either nucleus, but the values of μ calculated using an effective value of $g_s = 3.50$, as recommended by Covello and Sartoris,² are in good agreement with the experimental values.⁵ The magnetic moment of the first excited state in ^{203}Tl shows the opposite trend, being re-

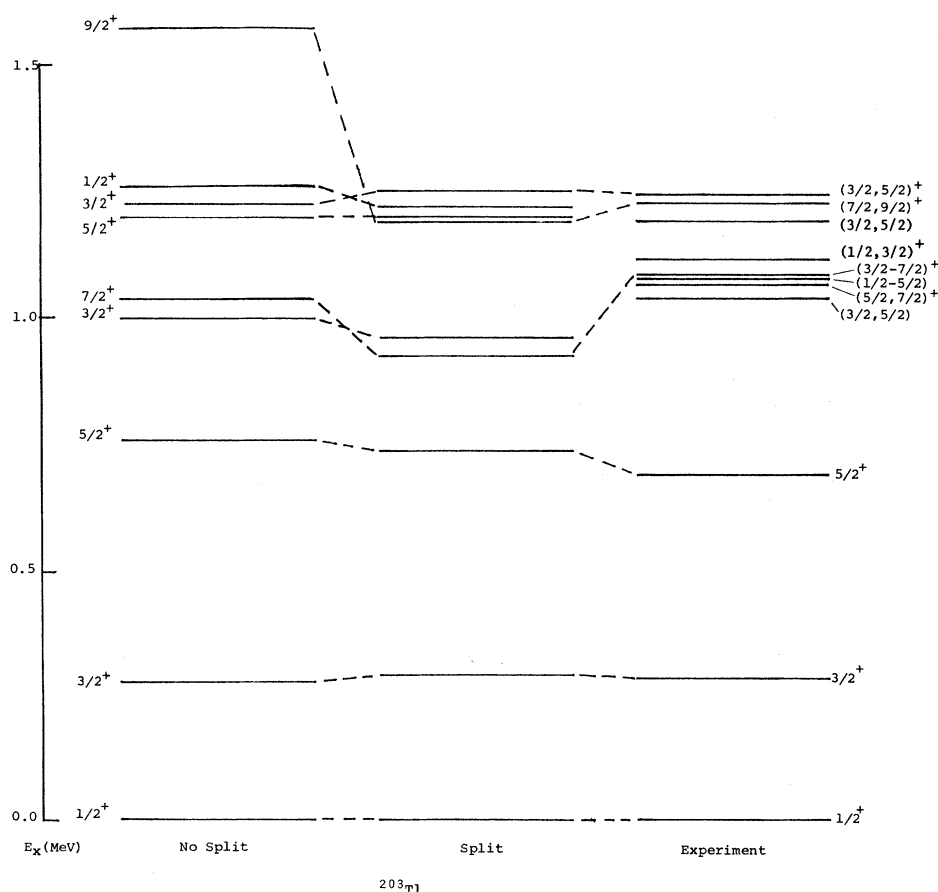


FIG. 8. The theoretical and experimental level schemes of ^{203}Tl are shown. The theoretical levels are from ICM calculations for the cases of nonsplit and split vibrational multiplets in the ^{204}Pb core and the experimental level scheme is from the combined results of the present and previous (Ref. 5) works.

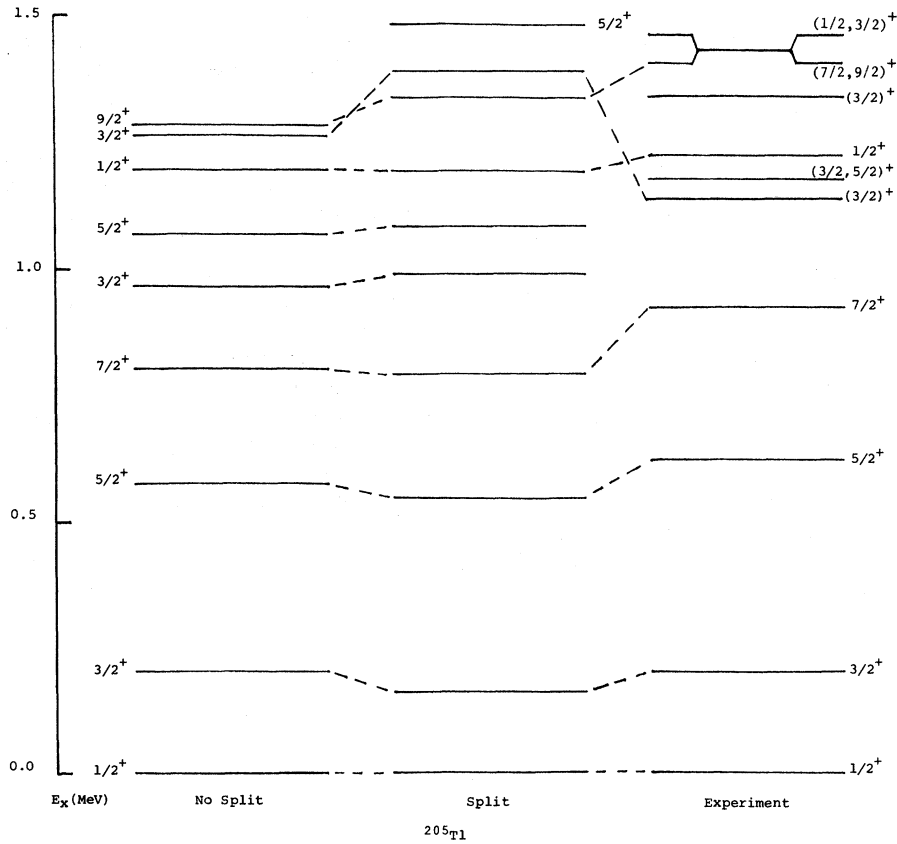


FIG. 9. The theoretical and experimental level schemes of ^{205}Tl are shown. The notation is as in Fig. 8.

TABLE V. Theoretical and experimental static moments.

$(J^\pi)_i$ ^a	$g_s = 5.58$		μ (μ_N) $g_s = 3.50$		Experiment ^b	Q (b) $e_p = 1.0$	
	Not split	Split	Not split	Split		Not split	Split
^{203}Tl							
$(\frac{1}{2}^+)_1$	2.694	2.720	1.674	1.695	1.6115		
$(\frac{3}{2}^+)_1$	-0.10	-0.06	0.512	0.557	0.16	0.295	0.243
$(\frac{5}{2}^+)_1$	3.507	3.382	2.507	2.402		0.131	0.077
$(\frac{7}{2}^+)_1$	0.505	0.278	1.188	0.939		0.296	0.171
^{205}Tl							
$(\frac{1}{2}^+)_1$	2.567	2.485	1.578	1.515	1.6274		
$(\frac{3}{2}^+)_1$	-0.271	-0.329	0.330	0.267		0.509	0.737
$(\frac{5}{2}^+)_1$	3.372	3.364	2.404	2.401		0.397	0.708
$(\frac{7}{2}^+)_1$	0.315	0.286	1.022	1.005		0.530	0.807

^a The notation is as in Table IV.

^b The experimental values of μ are from Ref. 5.

produced better for $g_s = 5.58$. No experimental information is available on quadrupole moments for these nuclei. The experimental lifetimes for the first two excited states are reasonably well reproduced, with the exception of the first excited state of ^{203}Tl , for which the calculated lifetime is an order of magnitude too large. Again the modification of the ICM to account for the splitting of the core multiplets fails to improve the calculated values. The predicted multipole mixing ratios for the γ -ray decays of the first and second excited states are in excellent agreement with the experimental values deduced in this and previous works.⁵

Above the second excited state, the correspondence of experimental to theoretical levels is less obvious, but based on the results of this and previous works we identify several levels in this region of excitation with ones predicted by the ICM. The $\frac{7}{2}^+$ state at 925 keV excitation in ^{205}Tl is clearly the predicted $\frac{7}{2}^+$ third excited state in that nucleus, a conclusion reached also by Barnard *et al.*⁹ The corresponding $\frac{7}{2}^+$ state in ^{203}Tl may be either the 1066 or the 1075 keV state, with the 1075 keV state favored, because of the similarity in the strength of its population to that of the 925 keV state in ^{205}Tl (see Sec. IV A 4). The large $l_n = 0$ strength⁶ in $^{206}\text{Pb}(t, \alpha)$ for the ^{205}Tl state at 1220 keV excitation strongly suggests that it is the $\frac{1}{2}^+$ state predicted near this energy (see Table IV). The corresponding $\frac{1}{2}^+$ state in ^{203}Tl was not identified^{6,7} in $^{204}\text{Pb}(t, \alpha)$ or $^{204}\text{Pb}(d, {}^3\text{He})$, which is surprising in view of the large spectroscopic strength predicted for this state. The large $l_n = 2$ strength⁶ in $^{206}\text{Pb}(t, \alpha)$ for the 1141 keV state in ^{205}Tl strongly suggests that it is the $(\frac{3}{2}^+)_3$ state predicted by the ICM to occur in this region of excitation. The multipole mixing ratio for the 1141 – 204 keV transition, however, is not in agreement with the prediction for this state. The large $l_n = 2$ strength^{6,7} for the 1233 keV state in ^{203}Tl is consistent with its being either the $(\frac{3}{2}^+)_2$ or the $(\frac{3}{2}^+)_3$ state predicted by the ICM. Based on the excitation energy of 1233 keV, the $(\frac{3}{2}^+)_3$ state is favored, but the reported⁹ γ -ray branching ratios favor its being identified with the predicted $(\frac{3}{2}^+)_2$ state. A particularly interesting result of the modified-core ICM calculations is the prediction of a $\frac{9}{2}^+$ level in both ^{203}Tl and ^{205}Tl near 1250 keV excitation (see Figs. 8 and 9). This state does not appear in any earlier theoretical level schemes, except that of Alaga and Ialongo,³ where it is predicted to occur near 1.5 MeV excitation. Thus, it is interesting that in ^{203}Tl a state at 1230 keV was tentatively reported²⁷ in $^{205}\text{Tl}(p, t)$ to have $L = 4$, and in ^{205}Tl a state at 1430 keV was tentatively reported⁸ in $^{205}\text{Tl}(p, p')$ to have $\Delta L = 4$. Since there are relatively few states of such high spin expected in this

TABLE VI. Theoretical and experimental lifetimes (ps).

$(J^\pi)_i$ ^a	Theory		Experiment
	Not split	Split	
^{203}Tl			
$(\frac{3}{2}^+)_1$	1920	4800	278
$(\frac{5}{2}^+)_1$	1.72	2.27	4.3
$(\frac{1}{2}^+)_2$	0.55	0.80	
$(\frac{3}{2}^+)_2$	0.25	0.25	
$(\frac{5}{2}^+)_2$	3.69	4.76	
^{205}Tl			
$(\frac{3}{2}^+)_1$	1160	530	1500
$(\frac{5}{2}^+)_1$	1.27	0.91	1.66
$(\frac{1}{2}^+)_2$	0.26	0.46	
$(\frac{3}{2}^+)_2$	0.12	0.11	
$(\frac{5}{2}^+)_2$	0.65	0.41	

^a The subscript denotes whether the level is the first, second, etc., having that spin.

region of excitation, it is quite possible that these levels correspond to the $\frac{9}{2}^+$ states predicted by the ICM.

VII. SUMMARY AND CONCLUSION

In this work, the excited states of $^{203,205}\text{Tl}$ were studied using the $^{203,205}\text{Tl}(n, n'\gamma)$ reactions. Spins and spin limits were deduced for excited states in these nuclei as summarized in Figs. 2 and 3. ICM calculations were performed and the results were compared with the experimental results from this and earlier works. In general, the calculations qualitatively reproduced the proper number and density of levels as a function of excitation energy. The identification of specific levels in the experimental schemes with predicted ones was made as summarized in Figs. 8 and 9. The agreement between the predicted and measured properties of these states was generally good. A modification of the core Hamiltonian to account for the splitting of the two-phonon triplet was found to make little change in the overall quality of the ICM predictions. The greatest exception was in the case of the $\frac{9}{2}^+$ state of ^{203}Tl , for which the predicted excitation energy is over 300 keV too high in the normal ICM calculation, but is within 30 keV of the experimental value for the modified-core calculation. This behavior can be explained by the fact that the largest component in the wave function of this state is the two-phonon term $|24, \frac{1}{2}\rangle$, and therefore the effect of splitting the two-phonon

TABLE VII. Theoretical and experimental mixing ratios and branching ratios in $^{203,205}\text{Tl}$.

Transition ^a (J^π) _i → (J^π) _j	Arctan δ ^b		Experiment ^c	Branching ratio (%)		
	Not split	Split		Not split	Split	Experiment ^d
^{203}Tl						
($\frac{3}{2}^+$) ₁ → ($\frac{1}{2}^+$) ₁	-49	-41	-50 <u>5</u>			
($\frac{5}{2}^+$) ₁ → ($\frac{1}{2}^+$) ₁				28	25	19
→ ($\frac{3}{2}^+$) ₁	-1	-1	-2 <u>8</u>	72	75	81
($\frac{1}{2}^+$) ₂ → ($\frac{1}{2}^+$) ₁				75	74	
→ ($\frac{3}{2}^+$) ₁	-68	-68		25	26	
→ ($\frac{5}{2}^+$) ₁				0	0	
($\frac{3}{2}^+$) ₂ → ($\frac{1}{2}^+$) ₁	85	87		45	37	
→ ($\frac{3}{2}^+$) ₁	16	10		18	18	
→ ($\frac{5}{2}^+$) ₁	1	0		37	45	
($\frac{5}{2}^+$) ₂ → ($\frac{1}{2}^+$) ₁				4	4	
→ ($\frac{3}{2}^+$) ₁	-75	89		94	87	
→ ($\frac{5}{2}^+$) ₁	-19	-6		3	9	
($\frac{3}{2}^+$) ₃ → ($\frac{1}{2}^+$) ₁	-46	-28		2	2	42 ^e
→ ($\frac{3}{2}^+$) ₁	-36	-46		3	4	36 ^e
→ ($\frac{5}{2}^+$) ₁	-87	-87		95	94	22 ^e
^{205}Tl						
($\frac{3}{2}^+$) ₁ → ($\frac{1}{2}^+$) ₁	-50	-55	-60 <u>22</u>			
($\frac{5}{2}^+$) ₁ → ($\frac{1}{2}^+$) ₁	-3	-5	-5 <u>7</u>	31	43	10
→ ($\frac{3}{2}^+$) ₁				69	57	90
($\frac{1}{2}^+$) ₂ → ($\frac{1}{2}^+$) ₁				54	38	85
→ ($\frac{3}{2}^+$) ₁	-74	-78		44	59	15
→ ($\frac{5}{2}^+$) ₁				2	3	0
($\frac{3}{2}^+$) ₂ → ($\frac{1}{2}^+$) ₁	81	82		49	54	
($\frac{3}{2}^+$) ₁	51	70		29	36	
($\frac{5}{2}^+$) ₁	9	20		22	10	
($\frac{5}{2}^+$) ₂ → ($\frac{1}{2}^+$) ₁				11	23	
→ ($\frac{3}{2}^+$) ₁	88	-89		84	73	
→ ($\frac{5}{2}^+$) ₁	-46	-65		5	4	
($\frac{3}{2}^+$) ₃ → ($\frac{1}{2}^+$) ₁	-74	-81	-88 <u>22</u>	38	53	22
($\frac{3}{2}^+$) ₁	-26	-26	(-89 <u>13</u>)	48	37	62
($\frac{5}{2}^+$) ₁			(14 <u>13</u>)	14	10	16

^a The notation is as in Table IV.

^b Arctan δ is given in degrees.

^c Experimental values of the mixing ratios are from the present work.

^d Experimental values of the branching ratios are from Ref. 9.

^e These branching ratios suggest that the 1233 keV level of ^{203}Tl may actually correspond to the ($\frac{3}{2}^+$)₂ theoretical level. Its identification as the ($\frac{3}{2}^+$)₃ theoretical level was based on its excitation energy and spectroscopic factor (see Table IV).

triplet is large. In the case of states of lower spin in the same region of excitation, the zero- and one-phonon terms dominate the wave functions, and the effect of splitting the two-phonon triplet is small. Interestingly, the corresponding $\frac{3}{2}^+$ state in ^{205}Tl is little affected by the introduction of core

splitting. This is because very little change occurs in the position of the 4^+ member of this multiplet in ^{206}Pb when the core Hamiltonian is modified.

We thank T. Newton for his assistance in collecting the data.

† This work was supported in part by the National Research Council of Canada.

* Present address: W. K. Kellogg Radiation Laboratory, California Institute of Technology, Pasadena, California 91125.

¹L. Silverberg, *Ark. Fys.* **20**, 355 (1961).

²A. Covello and G. Sartoris, *Nucl. Phys.* **A93**, 481 (1967).

³G. Alaga and G. Iolongo, *Nucl. Phys.* **A97**, 600 (1967).

⁴N. Azziz and A. Covello, *Nucl. Phys.* **A123**, 681 (1969).

⁵R. L. Auble, *Nucl. Data* **B5**, 531 (1971); M. R. Schmorak, *ibid.* **B6**, 425 (1975).

⁶S. Hinds, R. Middleton, J. H. Bjerregaard, O. Hansen, and O. Nathen, *Nucl. Phys.* **83**, 17 (1966).

⁷D. Royer, M. Arditi, L. Bimbot, H. Doubre, N. Frascaria, J. P. Garson, and M. Riou, *Nucl. Phys.* **A158**, 516 (1970).

⁸C. Glashauser, reported as a private communication in Ref. 5.

⁹E. Barnard, N. Coetzee, J. A. M. de Villiers, D. Reitmann, and P. van der Merwe, *Nucl. Phys.* **A157**, 130 (1970).

¹⁰N. Ahmed, D. R. Gill, W. J. McDonald, G. C. Nielson, and W. K. Dawson, *Phys. Rev. C* **11**, 869 (1975).

¹¹R. Moreh and A. Wolf, *Phys. Rev.* **182**, 1236 (1969).

¹²R. Moreh, A. Nof, and A. Wolf, *Phys. Rev. C* **2**, 249 (1970).

¹³R. Cesareo, M. Giannini, P. R. Olivia, D. Prospero, and M. C. Ramorino, *Nucl. Phys.* **A141**, 561 (1970).

¹⁴J. M. Davidson, H. R. Hooper, D. M. Sheppard, and G. C. Nielson, *Bull. Am. Phys. Soc.* **20**, 1155 (1975), J. M. Davidson, H. R. Hooper, P. W. Green, D. M. Sheppard, and G. C. Neilson, *Bull. Am. Phys. Soc.* **21**,

815 (1976); D. M. Sheppard, J. M. Davidson, H. R. Hooper, P. W. Green, and G. C. Neilson, in *Proceedings of the International Conference on Selected Topics in Nuclear Physics*, Dubna, USSR, 1976 (unpublished).

¹⁵J. M. Davidson, H. R. Hooper, D. M. Sheppard, and G. C. Neilson, *Nucl. Instrum. Methods* **134**, 291 (1976).

¹⁶J. M. Davidson, Internal Report No. 79, Nuclear Research Centre, University of Alberta, 1975 (unpublished).

¹⁷E. Sheldon and D. M. van Patter, *Rev. Mod. Phys.* **38**, 143 (1966).

¹⁸D. Wilmore and P. E. Hodgson, *Nucl. Phys.* **55**, 673 (1964).

¹⁹P. M. Endt and C. van der Leun, *At. Data Nucl. Data Tables*, **13**, 67 (1974).

²⁰D. W. O. Rogers, *Nucl. Instrum. Methods* **127**, 253 (1975).

²¹H. J. Rose and D. M. Brink, *Rev. Mod. Phys.* **39**, 306 (1967).

²²From the *Summary of Bases for Spin and Parity Assignments*, given in the preface of all issues of *Nuclear Data*.

²³B. Castel, K. W. C. Stewart, and M. Harvey, *Nucl. Phys.* **A162**, 273 (1971).

²⁴M. R. Schmorak and R. L. Auble, *Nucl. Data* **B5**, 207 (1971).

²⁵M. J. Martin, *Nucl. Data* **B5**, 601 (1971); K. K. Seth, *ibid.* **B7**, 161 (1972).

²⁶C. M. Lederer, J. M. Hollander, and I. Perlman, *Tables of Isotopes* (Wiley, New York, 1967).

²⁷T. Cleary, C. King, P. R. Mauronzig, and N. Stein, reported as a private communication in Ref. 5.